

Time Characteristics of High-Speed Fracture of Composite Building Materials at High Temperatures

N. S. Selyutina^{a, b, *} (ORCID: 0000-0002-6994-8663) and D. D. Khairetdinova^b

^a St. Petersburg State University, St. Petersburg, 199034 Russia

^b Institute for Problems in Mechanical Engineering, Russian Academy of Sciences, St. Petersburg, 119178 Russia

*e-mail: nina.selutina@gmail.com

Received July 15, 2025; revised August 25, 2025; accepted September 15, 2025

Abstract—The dynamic strength of concretes under different temperature-velocity conditions is analyzed using the incubation time criterion and the thermal fluctuation theory of strength. The model is validated through comparison with experimental data on concrete with basalt and limestone aggregate. It is shown that the characteristic relaxation time of concrete increases within the temperature interval of 20 to 800°C and decreases at temperatures above ~800°C.

Keywords: dynamic strength, characteristic time, temperature, strain rate, activation energy

DOI: 10.1134/S1062873825714023

INTRODUCTION

Temperature and strain rate are key parameters affecting the quasi-static and dynamic strength of concrete. With an increase in the rate of deformation and a fixed temperature, a positive velocity sensitivity of the material is observed, i.e. the dynamic strength increases with the rate of deformation and exceeds the value of static strength. Furthermore, for certain types of concrete [1, 2], the commonly held view that both static and dynamic strength decrease with rising temperature above room temperature [3] does not consistently hold across all temperature ranges. In such cases, the quasi-static and dynamic strength of concrete [1, 2] decreases from room temperature to 200°C, increases from 200 to 400°C, decreases from 400 to 600°C and then decreases again. However, even at these higher temperatures, the strength remains greater than at 200°C, relative to the values measured at room temperature.

At constant temperature during high-speed deformation [4–6], the water content in the samples influences the strength of concrete. Concrete with 0% water saturation exhibits higher strength under static loads, and water-saturated concrete demonstrates greater strength under dynamic loads. Under static conditions, the phenomenon can be attributed to hydrostatic pressure in water-saturated concrete samples. Conversely, under dynamic conditions, the influence of hydrostatic pressure on concrete strength increases, which leads to a slowdown in the incubation processes during micro-cracking.

In this paper, a method is proposed for predicting the increase in both static and dynamic strength of concrete with rising temperature, based on the incubation time criterion [4, 7, 8], while incorporating the thermofluctuation mechanism of fracture [9–14]. By introducing the concept of incubation time and applying the standard equations of thermofluctuation strength theory, the model enables estimation of a material's dynamic strength across a wide range of deformation rates and temperatures. The proposed model demonstrates good predictive capability for the strength of concrete containing limestone and basalt aggregates under varying thermal and speed conditions. It is shown that the characteristic relaxation time decreases with increasing temperature up to approximately 1000 K, after which it begins to increase—an anomalous behavior for this parameter.

INCUBATION TIME CRITERION

The instability of strength characteristics in brittle materials under high-speed deformation has been observed in dynamic experiments involving rocks and concrete [2, 15]. Predicting the distinctive strain rate dependence of material strength across a wide range of strain rates remains one of the central challenges in fracture dynamics. In this paper, a structural-temporal approach—previously proposed in studies [4, 7, 8]—is employed to calculate material strength at varying strain rates. Dynamic strength σ_d is defined as the maximum value of the ultimate stress achieved in a sample when it is loaded until fracture. Within the

framework of the structural–temporal approach, the fracture condition is expressed as follows:

$$\frac{1}{\tau} \int_{t-\tau}^t \left(\frac{\sigma(t')}{\sigma_c} \right)^\alpha dt' \leq 1, \quad (1)$$

where τ is the incubation time of fracture, $\sigma(t)$ is the time dependence of the stresses in the sample (at the place of fracture), σ_c is the static compressive strength, α is the parameter characterizing the sensitivity of the material to the level of force field intensity that causes compression fracture. Within the framework of the structural-temporal approach, when determining the ultimate strength σ_u , condition (1) is written for each of the loads. In this case, the set of material characteristics α, τ, σ_c differs for the cases of tension and compression. In this work, the strain rate dependence of the compressive strength of concrete is considered. The fracture time t_* is determined from the condition in which the inequality (1) transforms into equality. The incubation time is the characteristic time of relaxation. In the case of fracture, the physical nature of the incubation time is associated with the relaxation processes of micro-cracking before macro-fracture.

Fracture criterion (1) implies the existence of an incubation period, preceding a macroscopic failure of the material. In this context, an incubation process is an essential component of the overall fracture process and occurs under both quasi-static and fast impact loads. The presence of this fracture incubation period gives rise to specific phenomena under dynamic loading, most notably the well-established strain-rate dependence of material strength. As one of the simplest interpretations of the fracture incubation time, let us consider an example of fracture caused by a slow ($t_* \gg \tau$) linearly growing tensile stress $\sigma(t) = \dot{\sigma}tH(t)$, where $\dot{\sigma} = \text{const}$ and $H(t)$ is the Heaviside step function. Substituting linear expression for $\sigma(t)$ into (1), we can calculate the time to fracture $t_* = \sigma_c/\dot{\sigma} + 0.5\tau$ and a value of the critical stress at the moment of fracture $\sigma_u = \sigma(t_*) = \sigma_c + 0.5\dot{\sigma}t$, where σ_c is the tabulated value of the material static strength. In the case of very slow stress growth $\dot{\sigma}\tau/\sigma_c \ll 1$, the ultimate stress does not differ much from the static strength $\sigma_u \approx \sigma_c$. The obtained expressions show that according to (1) the material remains intact at the moment when the static strength limit is achieved $t_c = \sigma_c/\dot{\sigma}$. It is crucial that before the onset of the macroscopic rupture of the material, preparatory processes having a characteristic temporal period τ evolve in the material structure (Fig. 1).

The main advantage of using the structural-temporal approach is the introduction of the incubation time parameter, which is invariant with respect to the loading history $\sigma(t)$. According to the notion of the incubation time, two concrete specimens with different

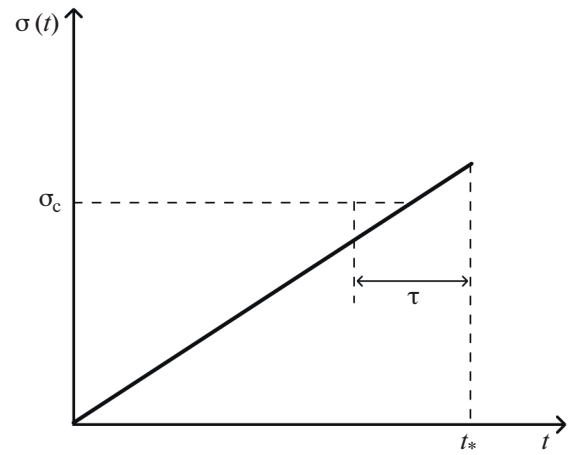


Fig. 1. Temporal dependence of stress for slow linear loading.

fibre volume fractions have different incubation time values. The incubation time is determined by approximation methods based on an experimental set of strength and strain rate values. The least squares method is used in this study. The loading of concrete samples in both static and dynamic experiments, as shown in the previous studies [4, 7, 8], is carried out according to the linear function of deformation in time.

The time dependence of the stresses in the sample has the following form:

$$\sigma(t) = E\dot{\epsilon}tH(t), \quad (2)$$

where E is Young’s modulus, $\dot{\epsilon}$ is the strain rate, and $H(t)$ is the Heaviside function. It is noted that wave processes are neglected when measuring the dynamic strength in experiments [1–3] on a split Hopkinson pressure bar, where long-term load pulses are set. Therefore, when assessing strength in a wide range of strain rates based on the structural-temporal approach (1), wave effects are also neglected.

Let us recall that, according to the given definition of strength above, for the case of linear loading, the strength is defined as $\sigma_u = \sigma(t_*) = E\dot{\epsilon}t_*$. Substituting (2) into the equality condition (1), the dependence of the fracture time on the strain rate $t_*(\dot{\epsilon})$ is determined:

$$t_*(\dot{\epsilon}) = \begin{cases} \left((\alpha + 1) \left(\frac{\sigma_c}{E\dot{\epsilon}} \right)^\alpha \tau \right)^{\frac{1}{\alpha+1}}, & \dot{\epsilon} \geq \sqrt[\alpha]{\alpha + 1} \frac{\sigma_c}{E\tau} \quad (t_* \leq \tau), \\ \frac{\sigma_u^{\text{sol}}}{(E\dot{\epsilon})^{\alpha+1}}, & \dot{\epsilon} < \sqrt[\alpha]{\alpha + 1} \frac{\sigma_c}{E\tau} \quad (t_* > \tau), \end{cases} \quad (3)$$

where σ_u^{sol} is the solution to the following equation with respect to σ_u :

$$(\sigma_u)^{\alpha+1} - (\sigma_u - E\dot{\epsilon}\tau)^{\alpha+1} = (\alpha + 1) E\dot{\epsilon}\tau\sigma_c^\alpha. \quad (4)$$

Then, by substituting the obtained dependence $t_*(\dot{\epsilon})$ (Eq. (3)) into σ_u , the dependence of the ultimate strength on the strain rate has the following form:

$$\sigma_u(\dot{\epsilon}) = \begin{cases} \left((\alpha + 1) E \dot{\epsilon} \tau \sigma_c^\alpha \right)^{\frac{1}{\alpha+1}}, & \dot{\epsilon} \geq \sqrt[\alpha]{\alpha + 1} \frac{\sigma_c}{E \tau} \quad (t_* \leq \tau), \\ \sigma_u^{\text{sol}}(\dot{\epsilon}), & \dot{\epsilon} < \sqrt[\alpha]{\alpha + 1} \frac{\sigma_c}{E \tau} \quad (t_* > \tau). \end{cases} \quad (5)$$

In the case of $\alpha = 1$, Eq. (5) is written explicitly:

$$\sigma_u(\dot{\epsilon}, T) = \begin{cases} \sqrt{2E\dot{\epsilon}\tau(T)\sigma_c}, & \dot{\epsilon} \geq \frac{2\sigma_c}{E\tau(T)} \quad (t_* \leq \tau(T)), \\ \sigma_c + \frac{1}{2} E \dot{\epsilon} \tau(T), & \dot{\epsilon} < \frac{2\sigma_c}{E\tau(T)} \quad (t_* > \tau(T)). \end{cases} \quad (6)$$

Thus, Eq. (6) provides a simple description of the ultimate stress across a wide range of strain rates. To estimate the incubation time τ and the amplitude parameter α , the least squares method is used on a set of experimental data referring to critical stresses and corresponding strain rates. In the paper [7], the process of fracture within the framework of the structural-temporal approach, written at $\alpha = 1$, is considered at various scale levels, and the characteristic of τ is determined at a given scale level. Establishing a set of material parameters σ_c, E, τ makes it possible to construct a non-linear relationship.

HYBRID MODEL

In this section, we define the temperature dependencies for the characteristic relaxation time $\tau(T)$ and introduce them on the basis of the thermofluctuation theory of strength [12, 16, 17]. In this case, the intensity of the relaxation process is usually considered as a process with an exponential dependence on temperature [12]. The canonical form of the Zhurkov formula has the form [12]) for estimating the temperature dependence of the intensity of relaxation processes:

$$\tau(T) = \tau_a \exp\left(\frac{U_0 - \delta\sigma}{kT}\right), \quad (7)$$

where $\tau(T)$ is the effective time to reach a state close to equilibrium (such a movement of the system towards equilibrium is called relaxation) [12], τ_a is the period of oscillation of atoms in a solid ($\tau_a = 10^{-12} \dots 10^{-13}$ s), U_0 is the initial activation energy in the unstressed state of the body (the activation energy of interatomic bonds), δ is the structural coefficient that characterizes the velocity of decrease in activation energy with increasing stress under fracture, $k = 8.314$ J/(K mol) is the Boltzmann's universal gas constant. The value of

the barrier $U(T)$ under the assumptions presented in the work [18] is determined as:

$$U(T) = kT \ln\left(\frac{\tau_c}{\tau_a}\right), \quad (8)$$

where τ_c is the effective time to reach a state close to equilibrium (such movement of the system towards equilibrium is the relaxation) [12]. Equation (8) showed good agreement with experimental data in the papers [11, 19, 20] for concrete with sand aggregate in various temperature ranges from -40 to $+60^\circ\text{C}$ [11]; from -5 to -25°C [19]; from -40 to 0°C [20].

Based on studies on the long-term strength of concrete in the temperature range from -40 to $+60^\circ\text{C}$ in [18], it was established: (1) the activation energy of fracture is independent of applied stress and temperature and is equal to 162.8 kJ/mol; (2) the pre-exponential constant, which characterizes the average time between successive thermal oscillations, depends on both stress and temperature; the higher the temperature, the less the effect of stress. In [18], it was proposed to use Zhurkov's formula Eq. (7) in the following generalized form:

$$\tau(T) = \tau_a \sigma(T) \exp\left(\frac{U_0}{kT}\right). \quad (9)$$

In [21], Zhurkov's formula (Eqs. (7) and (9)) and the structural-time approach were applied to determine the strength dependencies during spall fracture:

$$\tau(T) = \tau_a \exp\left(\frac{U_0 - \delta\sigma}{kT}\right) - \frac{t_i}{2}, \quad (10)$$

where t_i is the pulse duration. In this paper, the intensity of the relaxation process is proposed to be written as decreasing and increasing exponential dependencies:

$$\tau(T) = \tau_a \exp\left(\frac{U_0}{kT}\right) + \tau_1 \exp\left(\frac{T_m}{T - T_m}\right). \quad (11)$$

Here: T_m is the melting temperature of the aggregate material, τ_1 is constant material.

VELOCITY DEPENDENCIES OF THE STRENGTH OF CONCRETES WITH BASALT AND LIMESTONE AGGREGATE

Within the framework of the incubation time criterion, theoretical dependencies of strength on the strain rate were developed for concretes produced with limestone aggregate (concrete L) and with basalt aggregate (concretes B1 and B2), based on experimental data [1, 22]. Dynamic and static experiments on compressive strength in [1, 22] were carried out at different fixed temperatures: 20, 400, 650, 800, and 950°C for concrete with basalt aggregate [22] and 20, 200, 400, 600, and 800°C for concrete with limestone aggregate [1]. For each temperature illustrated in Fig. 2, two theoretical strength dependencies on strain rate were

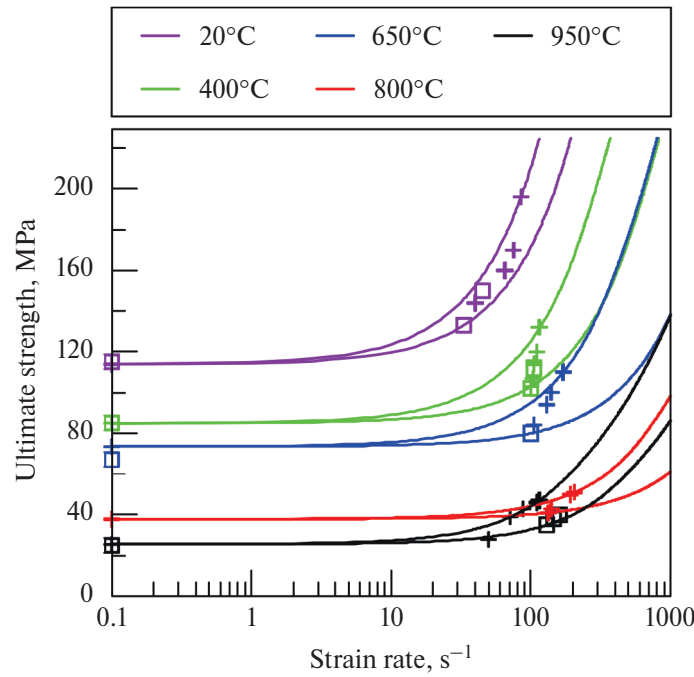


Fig. 2. The range of theoretical speed dependencies of concrete strength at different temperatures, plotted on experimental data by tests of concrete B1 [22] and B1 [22].

plotted, indicated by solid lines: one curve intersected the minimum experimental point $(\dot{\epsilon}, \sigma_u)$, while the other aligned with the maximum experimental point $(\dot{\epsilon}, \sigma_u)$. As a result, the range of experimental values $(\dot{\epsilon}, \sigma_u)$ was between these two theoretical dependencies. The values of Young’s modulus and static strength for each temperature are set according to experimental data [1, 22] from stress–strain relationships and take a fixed value for each temperature. The two theoretical dependencies of strength on the strain rate for concretes B1, B2 and L differed only in the fracture characteristic time, thereby setting the characteristic time interval for each temperature: from 80.8 to 135.4 μs at 20°C; from 42.35 to 95 μs at 400°C; from 19.4 to 64.1 μs at 650°C; from 17.4 to 47.67 μs at

800°C; from 88.6 to 227.3 μs at 950°C for concretes B1 and B2 and from 39.9 to 97.1 μs at 20°C, from 60.1 to 82 μs at 200°C, from 122.5 to 157.86 μs at 400°C, from 78.6 to 181.46 μs at 600°C, from 247.2 to 350.8 μs at 800°C for concrete L. For the entire set of experimental values $(\dot{\epsilon}, \sigma_{ul})$, the parameter of the average characteristic time is also determined for both concretes: 113.4 μs at 20°C; 72.62 μs at 400°C; 49.5 μs at 650°C; 39.4 μs at 800°C; 148.5 μs at 950°C for concretes B1 and B2 and at 68.5 μs 20°C, 72.65 μs at 200°C, 139.65 μs at 400°C, 129.65 μs at 600°C, 307.55 μs at 800°C for concrete L.

We develop the temperature dependence of the incubation time using a hybrid model of Eq. (11) for the derived range of characteristic times, on the basis

Table 1. Mix proportions of concrete [1, 22]

Designation for this work	Concrete B1	Concrete B2	Concrete L
Reference	[22] (concrete C)	[22] (concrete B)	[1]
Water, kg/m ³	166	179	180
Cement, kg/m ³	442	391	371
Fly ash, kg/m ³	78	69	99
Sand, kg/m ³	689	689	672
Admixture, kg/m ³	5.3	3.5	5
Rubble, kg/m ³	1125	1172	1008
Material of rubble	Basalt	Basalt	Limestone

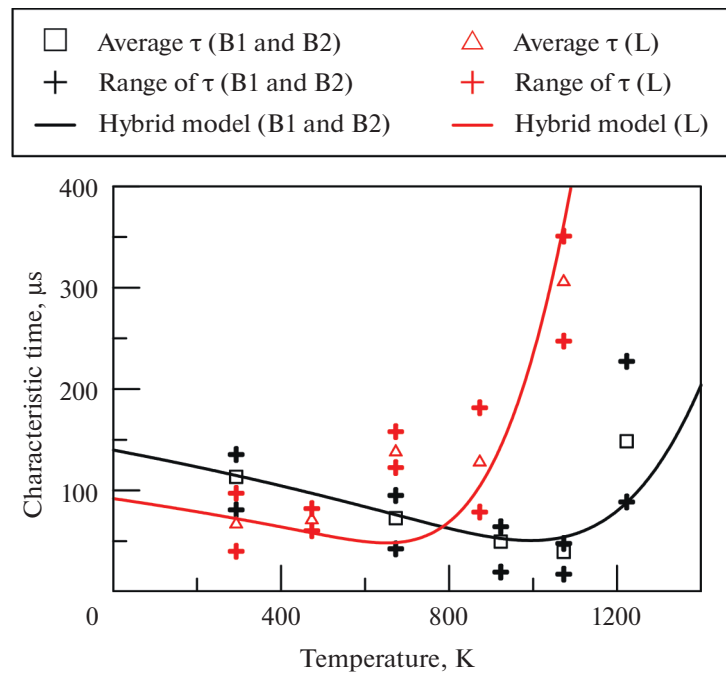


Fig. 3. Temperature dependences of the characteristic time of concrete B1, B2 and L.

of which the theoretical dependences of strength on the strain rate were calculated in Fig. 2. Parameters for the theoretical temperature dependences of characteristic time: (black curve, B1 and B2) $\tau_1 = 380 \mu\text{s}$, $U_0 = 2374 \text{ kJ/mol}$, $T_m = 1773 \text{ K}$ and $\tau_1 = 250 \mu\text{s}$, $U_0 = 195.3 \text{ kJ/mol}$, $T_m = 1500 \text{ K}$ (red curve, concrete L). The obtained values of the activation energy for concrete are close to the value $U_0 = 162.8 \text{ kJ/mol}$ obtained in [18] for concrete. Under the selected parameters, the hybrid model (11) exhibits dual behavior: the first term leads to an exponential increase of the characteristic relaxation time depending on temperature, while the second term, associated with the material's melting temperature, causes its decrease. Since the melting temperature of basalt exceeds that of limestone, the critical temperature at which the decreasing temperature dependence of the incubation time transitions to an increasing one is higher for concrete with basalt aggregate than for concrete with limestone aggregate. As shown in Fig. 3, the incubation time for concrete with limestone aggregate increases with temperature, whereas for concrete with basalt aggregate, it initially decreases up to 800°C and then increases. It should be noted that the decrease in the theoretical dependence of the characteristic relaxation time on temperature for limestone-containing concrete, modeled using the hybrid approach, falls within the permissible range of incubation time values indicated by the data points at 20 and 200°C , from room temperature up to 200°C . The proposed hybrid model requires further development to accurately predict the observed increase in incubation time within the temperature range of 200 to

400°C , as well as its subsequent decrease from 400 to 600°C .

At high temperatures, the influence of inertial forces on the strength of the concrete is dominant, since the concrete structure has more cracks and an increased water content. The latter effect, combined with inertial forces, makes it possible to increase the characteristic and dynamic strength at the same time. The resulting effect is considered anomalous because the typical dependence at high temperatures is a decreasing function of relaxation time.

CONCLUSIONS

The proposed model accurately predicts the strength of concrete with limestone and basalt aggregates under varying temperature and loading rate conditions. Based on the incubation time criterion and the principles of the thermofluctuation theory of strength, two distinct temperature-dependent relationships for the characteristic time were developed: one for concrete with limestone aggregate and another for concrete with basalt aggregate. The results show that both the rate of increase in dynamic strength and the characteristic relaxation time are influenced by the type of aggregate.

FUNDING

The study was supported by the Ministry of Science and Higher Education of the Russian Federation, agreement number no. 075-15-2022-1114. N.S. Selyutina performed

her part of the work with the support of the Ministry of Science and Higher Education of the Russian Federation (project no. 124041500007-4).

CONFLICT OF INTEREST

The authors of this work declare that they have no conflicts of interest.

REFERENCES

1. Su, H., Xu, J., and Ren, W., *Mater. Des.*, 2014, vol. 56, p. 579.
<https://doi.org/10.1016/j.matdes.2013.11.024>
2. Li, L., Zhang, R., Jin, L., Du, X., Wu, J., and Duan, W., *Constr. Build. Mater.*, 2019, vol. 210, p. 673.
<https://doi.org/10.1016/j.conbuildmat.2019.03.138>
3. Chen, L., Fang, Q., Jiang, X., Ruan, Z., and Hong, J., *Int. J. Impact Eng.*, 2015, vol. 86, p. 40.
<https://doi.org/10.1016/j.ijimpeng.2015.07.002>
4. Selyutina, N.S. and Petrov, Y.V., *Eng. Fract. Mech.*, 2020, vol. 225, p. 106265.
<https://doi.org/10.1016/j.engfracmech.2018.11.052>
5. Selyutina, N. and Smirnov, I., *Mech. Mater.*, 2023, vol. 179, p. 104613.
<https://doi.org/10.1016/j.mechmat.2023.104613>
6. Selyutina, N.S. and Khairtdinova, D.D., *J. Dyn. Behav. Mater.*, 2025, vol. 11, p. 34.
<https://doi.org/10.1007/s40870-024-00424-y>
7. Petrov, Yu.V., Gruzdkov, A.A., and Bratov, V.A., *Phys. Mesomech.*, 2012, vol. 15, no. 2, p. 232.
<https://doi.org/10.1134/S1029959912020117>
8. Petrov, Y.V., Smirnov, I.V., Volkov, G.A., Abramian, A.K., Bragov, A.M., and Verichev, S.N., *J. Rock Mech. Geotech. Eng.*, 2017, vol. 9, no. 1, p. 125.
<https://doi.org/10.1016/j.jrmge.2016.09.004>
9. Kartashov, E.M., *Fine Chem. Technol.*, 2021, vol. 16, no. 6, p. 526.
<https://doi.org/10.32362/2410-6593-2021-16-6-526-540>
10. Kovshov, A.G., *Izv. Samar. Nauchn. Tsentra Ross. Akad. Nauk*, 2020, vol. 22, no. 3, p. 37.
<https://doi.org/10.37313/1990-5378-2020-22-3-37-43>
11. Iskakbayev A.I., Teltayev B.B., Yestayev K.Z., and Abu, B.D., *Constr. Build. Mater.*, 2020, vol. 244, p. 118325.
<https://doi.org/10.1016/j.conbuildmat.2020.118325>
12. Solov'eva, Y.V., Starenchenko, S.V., and Starenchenko, V.A., *Bull. Russ. Acad. Sci.: Phys.*, 2020, vol. 84, p. 1582.
<https://doi.org/10.3103/S1062873820110258>
13. Goldenberg, B.G., Rakshun, Y.V., Bugaev, S.V., Meshkov, O. I., and Tsybulya, S.V., *Bull. Russ. Acad. Sci.: Phys.*, 2019, vol. 83, p. 129.
<https://doi.org/10.3103/S1062873819020151>
14. Glebovskii, P.A. and Petrov, Yu.V., *Phys. Solid State*, 2004, vol. 46, p. 1051.
<https://doi.org/10.1134/1.1767243>
15. Su, H., Xu, J., and Ren, W., *Mater. Des.*, 2014, vol. 56, p. 579.
<https://doi.org/10.1016/j.matdes.2013.11.024>
16. Zhurkov, S.N., *Izv. Akad. Nauk SSSR, Ser. Inorg. Mater.*, 1967, vol. 3, no. 10, p. 1767.
17. Regel, V.R., Slutsker, A.I., and Tomashevskiy, E.Ye., *Kineticheskaya priroda prochnosti tverdykh tel* (Kinetic Nature of Solid Body Strength), Moscow: Nauka, 1974.
18. Slutsker, A.I., Polikarpov, Y.I., and Vasil'eva, K.V., *Phys. Solid State*, 2002, vol. 44, p.1604.
<https://doi.org/10.1134/1.1501366>
19. Gubach, L.S. and Fisher, E.K., *Mezhvuzovskii sbornik* (Interuniversity Collection), 1979, p. 3.
20. Nickolskiy, Yu.E., Pisklin, V.M., and Shestakov, V.N., *Mezhvuzovskii sbornik* (Interuniversity Collection), 1979, p. 10. (In Russian).
21. Zhurkov, S.N., *Fiz. Tverd. Tela*, 1980, vol. 22, no. 11, p. 3344.
22. Chen, L., Fang, Q., Jiang, X., Ruan, Z., and Hong, J., *Int. J. Impact Eng.*, 2015, vol. 86, p. 40.
<https://doi.org/10.1016/j.ijimpeng.2015.07.002>

Publisher's Note. Pleiades Publishing remains neutral with regard to jurisdictional claims in published maps and institutional affiliations. AI tools may have been used in the translation or editing of this article.

SPELL: 1. ok